

Monitoring Soil Condition in the Northern Tibetan Plateau Using SSM/I Data

A. T. C. Chang

Goddard Space Flight Center, Greenbelt, MD 20771, U.S.A.

M. S. Cao

Academia Sinica, Lanzhou, China

A combination of a low 37 GHz brightness temperature and a negative 19 and 37 GHz spectral gradient can be an effective discriminant for frozen and thawed soil. SSM/I data for 1988 are used to study the freeze/thaw of soil in the Northern Tibetan Plateau, China. In this study, a previously derived freeze/thaw classification scheme was tested for this unique geographic location. It was found that the 37 GHz threshold needed to be refined for this region. It was also found that the 37 GHz emission is sensitive to the scattering centers embedded in the soil, which may account for the observed low brightness temperature. The selection of the 37 GHz brightness temperature threshold depends on the atmospheric and soil conditions inherent in a particular region.

Introduction

Microwave radiometry has been used to infer soil freeze/thaw condition with some success. The usefulness of the microwave techniques derive from the fact that the thermal microwave radiation emerging from an object depends on its physical temperature, composition and physical structure. It is the large contrast between the dielectric properties of water, soil and ice that make it possible to deduce the freeze/thaw condition of soil using microwave measurements.

Microwave remote sensing of the freeze/thaw condition of the soil has been reported by many authors. In determining the freeze/thaw condition of soil, Zuern-dorfer *et al.* (1990) used Nimbus-7 Scanning Multichannel Microwave Radiometer (SMMR) data to map daily freeze/thaw patterns in the upper Midwest for the fall of

1984. Wegmuller (1990) reported the effect of a frozen soil layer on the microwave signatures of bare soil. Zuerndorfer and England (1992) developed a freeze indicator, FI, based on a low 37 GHz brightness temperature and a low spectral gradient and applied the FI to classify frozen surfaces in the northern Great Plains.

The high elevation of the Tibetan Plateau exerts not only a strong barrier effect on the global atmospheric flow but also constitutes an elevated heat source that generates a temperature contrast with the surrounding free atmosphere. A growing body of modeling and observational evidence which suggests that the slowly varying surface boundary conditions, such as the freeze and thaw of soil in this region, can influence the interannual variability of the atmospheric circulation of this region and the Indian monsoon. Due to its remote geographic location, measurements of these surface parameters are not routinely made. So remote sensing data will be useful in supplementing the conventional observations.

A major challenge in the remote sensing of soil parameters is the development of a robust algorithm which can effectively delineate the freeze/thaw condition of the soil. In this paper we discuss the feasibility of using satellite passive microwave measurements to determine the physical state of soil on the Tibetan Plateau. The algorithm derived by Zuerndorfer *et al.* (1990) for monitoring soil condition is tested and refined using data from the Special Sensor Microwave/Imager (SSM/I) on board the Defense Meteorological Satellites.

Background

Microwave remote sensing of soil moisture relies on the large contrast between the dielectric constant of water (~ 30) and that of dry soil (3.5) at about 20 GHz. There is a strong dependence on the thermal emission from the soil and its moisture content. This dependence provides a means for remotely sensing the moisture content in a surface layer less than about 5 cm thick. The brightness temperature of soil measured by space-borne sensors can be approximated as (Ulaby *et al.* 1981)

$$T_B \equiv e T_0 + (1-e) T_{\text{sky}}$$

where e and T_0 are the emissivity and surface temperature of the ground, and T_{sky} is the effective sky brightness. For this study, we are ignoring the atmospheric emission and absorption effects in the 19 and 37 GHz brightness temperatures due to the high elevation of Tibetan Plateau ($> 4,000$ m).

Freezing influences the measured brightness temperature of the ground. Usually it will: 1) lower the thermal temperature, T_0 , 2) increase emissivity, e , due to tighter bounding of the free soil moisture, and 3) provide a negative brightness gradient, (Zuerndorfer *et al.* 1990). A lower T_0 will decrease the brightness temperature, and a tighter bounding of the soil moisture will increase the brightness temperature. Changes of brightness temperature that result from freezing may either be positive or negative, depending upon the soil moisture content. Thus the combination of 1)

and 2) may not be able to delineate frozen ground unambiguously.

The state of freeze and thaw of soil is not only important in determining the energy exchange between the air and ground through the latent heat of fusion and vaporization, but also important in inferring snow depth information. A two-parameter freeze indicator, FI has been reported by Zuerndorfer *et al.* (1990) using the Nimbus-7 Scanning Multichannel Microwave Radiometer (SMMR) data. The two parameters are 1) 37 GHz brightness temperature below 247 K, and 2) 10.7-37 GHz spectral gradient having a value lower than -0.3 K/GHz. The behavior of the 37 GHz brightness temperature and the dominant characteristics of the spectral gradient can be explained by a one dimensional half space, model for moist soil (England 1990). It has been generally acknowledged that FI is adequate to discriminate the frozen/thawed soil in areas of North Dakota.

The SSM/I is a four frequency (19.35, 22.235, 37 and 85.5 GHz) microwave radiometer in a near-polar sun-synchronous orbit, flown on a DMSP satellite. The spatial resolution varies from 69×43 km at 19.35 GHz to 15×13 km at 85.5 GHz. The antenna beams scan by continuous rotation with a period of 1.9 seconds along a conical surface with a vertical axis and a half angle of 45° , which intersects the earth's surface at an angle of 53° . It measures the radiation in both horizontal and vertical-polarizations at all frequencies except 22.235 GHz where it only measures the vertically polarized component. The swath width is about 1,400 km, and there will be gaps in the equatorial region. The first SSM/I was launched in June 1987 and since it is an operational instrument, one or more copies can be expected to be operating in orbit in the foreseeable future.

The SSM/I sensor system includes a 19.35 GHz channel rather than the 18 GHz in the SMMR. The absorption of water vapor by the atmosphere is slightly stronger for 19.35 GHz than for 18.0 GHz, thus 19.35 GHz should give a slightly higher brightness temperature. Due to the low humidity and high elevation of the Tibetan Plateau, the brightness difference between the 19.35 GHz and 18 GHz channels may be neglected.

In Zuerndorfer and England (1992), polarization was suppressed by averaging the vertical and horizontal components of the SMMR brightness temperature. For easier comparison, in this study we have also averaged the vertical and horizontal polarizations. Also, instead of using the 10-18-37 GHz spectral gradients (Zuerndorfer and England 1992), the 19.35-37 GHz spectral gradients are used.

Study Area

The Tibetan Plateau is about 2.5 million square km in size and about 70% of this area consists of high pastures. The desolate northern area (Chang Tang), north of about 32° N latitude, is mostly uninhabited or only sparsely populated. It is a place so remote that even nomadic herdsmen do not venture into it (Schaller 1993). The ground observation network in the Chang Tang area is thus limited. Remote sensing

may be the only way to monitor the soil and snow condition for this inaccessible area on a routine basis.

There is very sparse surface vegetation in this region; the coverage is usually less than 20% and the most common vegetation is *Stapa purpurea* and *Stipa subsessiliflora* grasses (Li 1993). The most widely distributed soil type is sand having less than 1% organic material; the surface soil moisture content is low most of the time. The average duration of sunshine is 3180 hours per year (over 8.5 hr/day). Due to the strong solar radiation, continuous winds and long durations of sunshine, surface evaporation is very high. Permafrost underlies much of this area at a depth of one to two metres. This region has more permafrost than any other mid-latitude area.

For this study, 1988 climatology data from Gerze station (32° 09'N, 84° 25'E) which is located at the edge of Chang Tang were used to represent the entire Northern Tibetan Plateau. The station is located 4,415 m above the mean sea level. The annual average temperature is 0.1 °C and annual precipitation is 166.1 mm. The maximum monthly mean temperature is 12.1 °C and minimum -11.9 °C (Li 1993). Most of the precipitation falls in the summer months, and the average snow cover is 30 days per year, with snow depth commonly less than 10 cm. For 1988 snow cover greater than 5 cm depth was reported from January 1 to February 1, and the maximum depth was 8 cm. Due to the low averaged relative humidity (annual average 33%) and sparse vegetation coverage, any amount of surface soil moisture will evaporate very quickly.

Microwave Observations

Figs. 1 (a,b) and 2 (a,b) show the SSM/I 19.35 and 37 GHz normalized brightness temperatures for a.m. and p.m. passes, respectively. Brightness temperatures within the one degree latitude by one degree longitude box (31° 30'N-32° 30'N; 84°E-85°E) centered at Gerze for the year of 1988 were plotted. Normalized brightness temperature is the measured brightness temperature divided by the 5 cm soil temperature and has the dimension of emissivity. 5-cm soil temperatures (Fig. 3) are used in this study, because most of the microwave radiation emitted by the surface emerges from the top layer (Zwally and Gloersen 1977). Diurnal heating will affect the 5 cm soil temperature slightly, so that there will be some difference in the normalized brightness temperature for the times of satellite pass (Zuerndorfer *et al.* 1990). The normalized emissivity for 37 GHz varies between 0.8 and 0.88 for the a.m. passes and between 0.84 and 0.9 for the p.m. passes. For 19.35 GHz, it varies between 0.82 and 0.9 for the a.m. passes and between 0.85 to 0.92 for the p.m. passes.

The sandy soil of this area is rather coarse (0.2 to 1.0 mm). A typical dielectric constant for dry sandy soil is about 3.0 and its emissivity based on Wang and Schmutge (1980) is about 0.93. The effect of volume scattering and soil moisture content at these wavelengths are the possible reason for the lower brightness values (England 1974).

Monitoring Soil Condition Using SSM/I Data

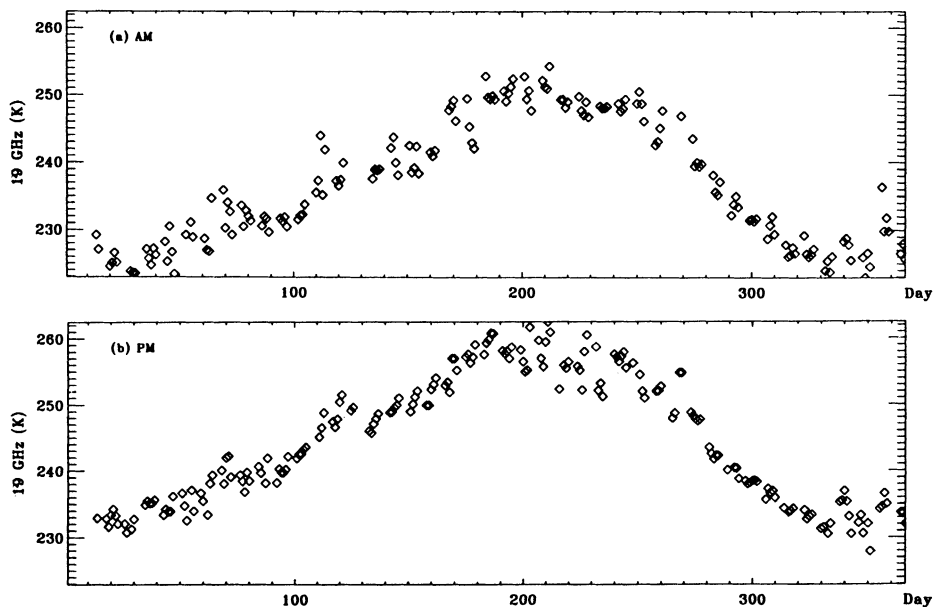


Fig. 1. Normalized 19 GHz brightness temperature versus day number of 1988 for Gerze station, (a) a.m. passes and (b) p.m. passes. Day 1 = January 1 and Day 366 = December 31.

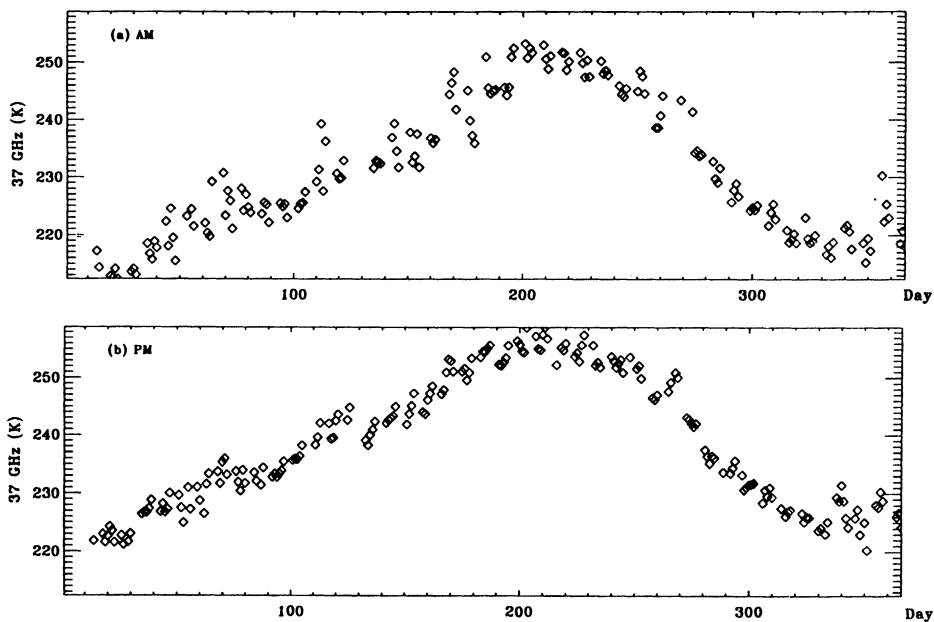


Fig. 2. Normalized 37 GHz brightness temperature versus day number of 1988 for Gerze station, (a) a.m. passes and (b) p.m. passes. Day number definition same as above.

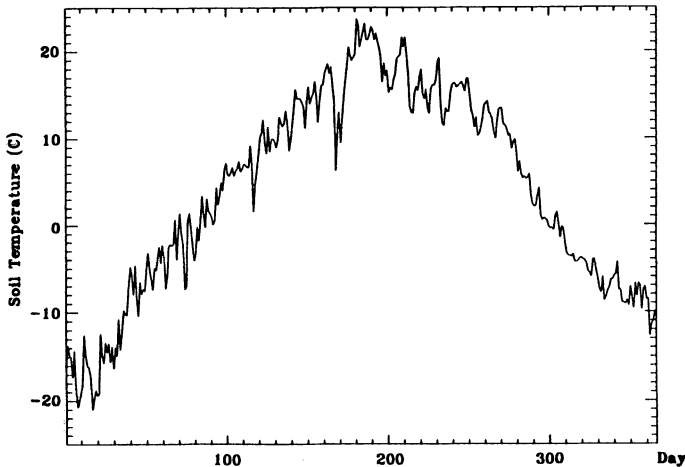


Fig. 3.
5 cm soil temperature
observed at Gerze station
for 1988.

The 37 GHz radiation, emerging mainly from the top layer of soil, could provide information on the soil temperature. A regression between soil temperature and 37 GHz brightness temperature gives a correlation coefficient of 0.9. However the standard error of estimate is 5.1 K, thus 37 GHz brightness alone may not be able to provide an accurate estimates whether or not the soil is frozen.

The normalized brightness temperatures of the a.m. passes are slightly lower than those of the p.m. passes for both of 19 and 37 GHz. This is likely due to the fact that the surface moisture at 6 a.m. is usually slightly higher than found at 6 p.m. due to percolation of moisture from the lower soil layer during the night before. The 19 GHz normalized brightnesses are systematically higher than those of the 37 GHz by a few per cent for both a.m. and p.m. This is probably due to the stronger volume scattering at 37 GHz, which results in a lower T_B .

When the soil freezes the normalized brightness increases due to the change in dielectric constant of water. The shift in emissivity with freezing is most pronounced at the lower microwave frequencies (Wegmuller 1990). At 19.35 and 37 GHz the effect is reduced but not absent (Zuerndorfer *et al.* 1990). Figs. 1 and 2 show no significant changes in the normalized brightness temperature when soil state changes from freeze to thaw and *vice versa*. This is due to the fact that the soil is mostly dry, thus there are no changes in the dielectric constant or the normalized brightness temperatures.

To evaluate the applicability of the FI for the Northern Tibetan Plateau, SSM/I data are used to derive the spectral gradient, and 37 GHz brightness are examined. Fig. 4 (a,b) shows the scatter plot of spectral gradient and soil temperature. All of the soil temperatures less than 0 °C had a spectral gradient less than -0.3 K/GHz. However there are many cases where soil temperatures greater than 0 °C also have a spectral gradient less than -0.3 K/GHz. A considerable amount of misclassification will result if one is using only the spectral gradient as the classifier.

Monitoring Soil Condition Using SSM/I Data

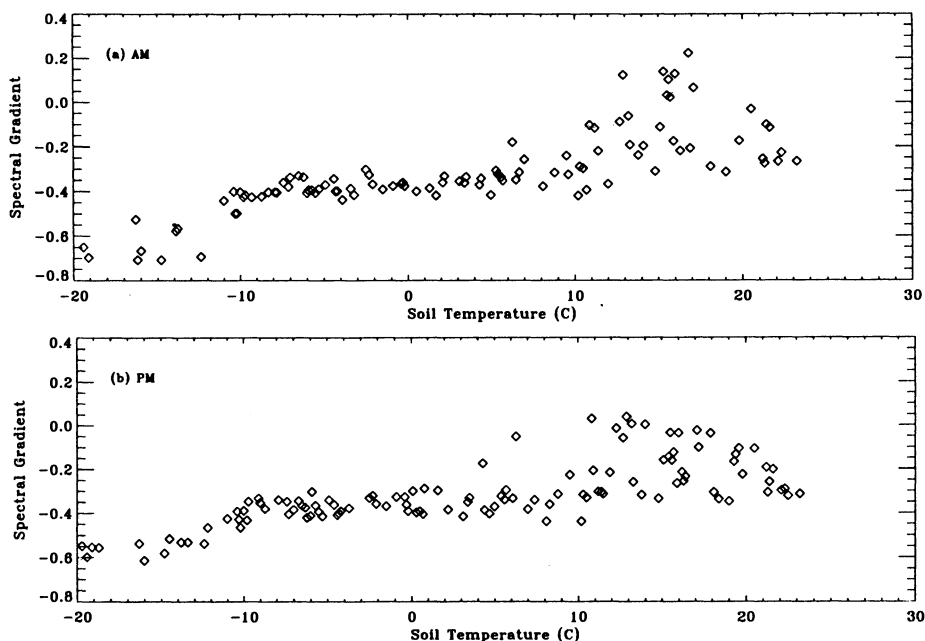


Fig. 4. Scatter plot of coincident microwave spectral gradient value and observed 5 cm soil temperature of Gerze station, 1988, (a) a.m. passes and (b) p.m. passes.

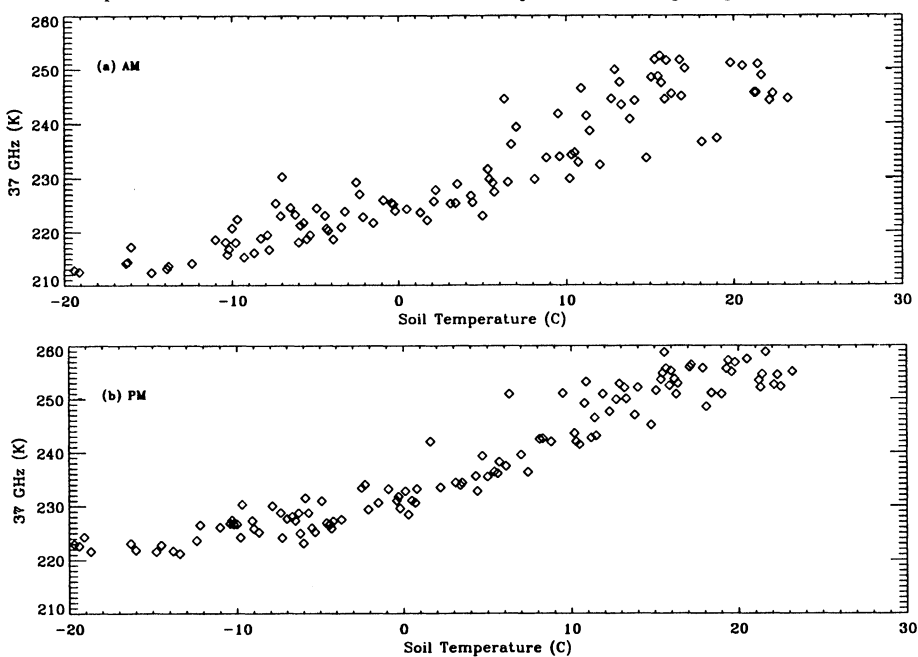


Fig. 5. Scatter plot of coincident observed 5 cm soil temperature and 37 GHz brightness temperature for Gerze station, 1988, (a) a.m. passes and (b) p.m. passes.

Fig. 5 (a,b) shows the scatter plot of 37 GHz brightness temperature and soil temperature for the a.m. and the p.m. passes. When the soil temperature was less than 0 °C, the 37 GHz brightness was lower than 231 K and 238 K for a.m. and p.m. passes, respectively. The 37 GHz brightness threshold of 247 K for frozen soil definitely needs to be refined for this area.

There are 175 observations for the a.m. passes and 202 observations for the p.m. passes. The classification results of the FI index are tabulated in Table 1. Typically, the FI classified the soil in January to May and October to December as frozen. Comparing with the ‘ground truth’, measured soil temperature, months of January to March and November and December soil temperatures were below 0°C (Fig. 3). FI misclassified the soil in the months of April, May and October.

To evaluate the classification technique, the following variables are commonly used: 1) F_F : number of points correctly classified as frozen ground (hits), 2) F_T : number of points incorrectly classified as frozen ground (missed), 3) T_F : number of points incorrectly classified as thawed ground, and 4) T_T : number of points correctly classified as thawed ground. When comparing with ‘truth’, the satellite-delineated frozen days can be expressed as

$$D_F = F_F + F_T$$

and ground-observed frozen days are denoted as G_F . Using the above variables, statistics have been devised in order to evaluate parameter estimation methods. The most commonly used are

The probability of detection = F_F / G_F

The false alarm rate = $1 - F_F / D_F$

The per cent error = $(T_F + F_T) / (F_F + T_F + F_T + T_T)$

Correct classification = $(T_T + F_F) / (F_F + T_F + F_T + T_T)$.

Table 1 – Classification results of Zuerndorfer *et al.* (1990) FI index

		SSM/I Derived	A.M. case		P.M. case	
Ground Truth		Freeze	Thaw	Ground Truth	Freeze	Thaw
	Freeze	70	2		75	0
	Thaw	43	60		59	68

Table 2 – Classification results of the modified FI index

		SSM/I Derived	A.M. case		P.M. case	
Ground Truth		Freeze	Thaw	Ground Truth	Freeze	Thaw
	Freeze	70	1		75	0
	Thaw	25	79		28	99

Monitoring Soil Condition Using SSM/I Data

The probability of detection gives a sense of the ability of the scheme to find the “freeze” case. However, a given scheme could create many more frozen soil cases than the actual, and still give a good probability of detection. A high probability of detection should be accomplished with a small false alarm rate in order to be meaningful. The per cent error is representative of the error in “freeze” delineation with respect to the total number of cases that the method is applied. The per cent error could be small even when the probability of detection is low and the false alarm rate is high, especially when there is a small number of freeze cases. For a more objective evaluation of the classification scheme, all statistics should be considered. The probability of detection, false alarm rate and per cent error are 0.97, 0.38 and 0.26 respectively for the a.m. passes. For p.m. passes, the respective values are 1.0, 0.44 and 0.29. Classification using the a.m. data seem to out-perform the p.m. data in both false alarm rate and per cent error.

By adopting 231 K and 238 K as the T_B threshold for the a.m. and the p.m. cases respectively, classification accuracy improved greatly. The classification results using these threshold are tabulated in Table 2. The per cent of correct classification improves from 74% to 85% for the a.m. case and 71% to 86% for the p.m. case. Incidentally, these brightness thresholds happened to be the mean annual brightness temperature for the grid box. We might be able to generalize the algorithm by selecting the annual mean brightness temperature as the threshold for different regions.

Frozen soil exhibits volume scatter decrease T_B at 19 and 37 GHz much like the effect observed in dry snow. England (1975) reported that this is probably due to imbedded ice lenses in the soil acting as scattering centers. When Grody (1991) used a scattering index to classify the Tibetan snow-covered area, more consistent snow cover values were derived. Grody also attributed this darkening to ice below the surface which scattered the microwave radiation. These scattering centers, probably part of the underlying permafrost layer, produce lower microwave signatures throughout the year. These signals might complicate the detection of the freeze/thaw state with snow cover. However, snow cover should not be a major factor, because in 1988, for example, only 30 snow covered days, with a few cm of snow was reported. With a shallow snow cover, the algorithms used in this study can accurately delineate the soil condition.

Summary

One year of SSM/I data and climatology data (1988) was used to evaluate and refine a method to infer the soil moisture state over the Tibetan Plateau. By using the negative spectral gradient and selected annual average of the 37 GHz brightness as threshold, the freeze and thaw states of soil can be classified to a 85% accuracy. Although SSM/I channels are different from those of the SMMR, with minor modification of the classification scheme, the freeze and thaw states of soil can be determined.

Snowpack could alter the microwave signatures sensed by space-born sensors. However, the shallow snow cover in the Tibetan Plateau will not affect the accuracy of this method.

References

- Chang, A. T. C., Foster, J. L., and Hall, D. K. (1987) Nimbus-7 SMMR derived global snow cover parameters. *Annals of Glaciology*, Vol. 9, 39-44.
- Chang, A. T. C. (1986) Nimbus-7 SMMR snow cover data, Glaciological Data Report GD-18, pp. 181-187.
- Chang, T. C., Gloersen, P., Schmugge, T. J., Wilheit, T. T., and Zwally, H. J. (1976) Microwave emission from snow and glacier ice, *Journal of Glaciology*, Vol. 16, pp. 23-39.
- England, A. W. (1974) Thermal microwave emission from a halfspace containing scatterers, *Radio Science*, Vol. 9, pp. 447-454.
- England, A. W. (1990) Radiobrightness of diurnal heated, freezing soil, *IEEE Trans GRS*, Vol. 28, pp. 464-475.
- Grody, N. C. (1991) Classification of snow cover and precipitation using the Special Sensor Microwave Imager, *Journal of Geophysical Research*, Vol. 96, pp. 7423-7435.
- Li, M. S. (1993) The utilization and Protection of the natural resources of the northern Tibet Plateau, *Journal of Natural Resources (in Chinese)*, Vol. 8, pp. 32-37.
- Schaller, G. B. (1993) Tibet's remote Chang Tang, *National Geographic*, Vol. 184, pp. 62-87.
- Ulaby, F. T., Moore, R. K., and Fung, A. K. (1981) *Microwave Remote Sensing, Active and Passive*, Addison-Wesley, Reading MA, pp 186-255.
- Wang, J. R., and Schmugge, T. J. (1980) An empirical model for the complex dielectric permittivity of soils as a function of water content, *IEEE Trans. Geoscience and Electronics*, Vol. GE-18, pp. 288-295.
- Wegmuller, U. (1990) The effect of freezing and thawing on the microwave signatures of bare soil, *Remote Sensing of Environment*, Vol. 33, pp. 123-135.
- Zuerndorfer, B., and England, A. W. (1992) Radiobrightness decision criteria for freeze/thaw boundaries, *IEEE Trans. Geoscience and Remote Sensing*, Vol. GRS-30, pp. 89-101.
- Zuerndorfer, B. W., England, A. W., Dobson, M. C., and Ulaby, F. T. (1990) Mapping freeze/thaw boundaries with SMMR data, *Agricultural and Forest Meteorology*, Vol. 52, pp. 199-225.
- Zwally, H. J., and Gloersen, P. (1977) Passive microwave images of the Polar regions and research applications, *Polar Record*, Vol. 18, pp. 431-450.

Received: 21 March, 1995

Accepted: 13 October, 1995

Address:

A. T. C. Chang,
Hydrological sciences Branch,
Laboratory for Hydrospheric Processes,
NASA, Goddard Space Flight Center,
Greenbelt, MD 20771, U.S.A.

M. S. Cao,
Lanzhou Institute of Glaciology and Geocryology,
Academia Sinica,
Lanzhou,
China.